PCCP

Accepted Manuscript

ROYAL SOCIETY OF CHEMISTRY

www.rsc.org/pccp

CREATED USING THE RSC LaTeX PCCP ARTICLE TEMPLATE – SEE www.rsc.org/electronicfiles FOR DETAILS

ARTICLE TYPE www. rsc.org/xxxxxx | XXXXXXXX

A new layered monoclinic phase of Co_3O_4 at high pressure

Thanayut Kaewmaraya,[a] Wei Luo,*[a] Xiao Yang,[a,b] Puspamitra Panigrahi[a] and Rajeev Ahuja[a,c]

Received Xth XXXXXXXXXX 20XX, Accepted Xth XXXXXXXXX 20XX

First published on the web Xth XXXXXXXXXX 200X

DOI: 10.1039/b000000x

We present the crystal structures and electronic properties of Co_3O_4 spinel under high pressure. Co_3O_4 undergoes a first-order transition from a cubic (CB) $Fd\bar{3}m$ to a lower-symmetry monoclinic (MC) $P2_1/c$ phase at 35 GPa, occurring after the local high-spin to low-spin phase transition. The high-pressure phase exhibits the octahedral coordination of Co(II) and Co(III), whereas the CB phase contains fourfold coordination of Co(II) and sixfold coordination of Co(III). The CB-to-MC transition is attributed to the charge-transfer between the di- and trivalent cations via the enhanced 3*d*-3*d* interactions.

1 Introduction

Co_3O_4 spinel has intrigued extensive research owing to its importances for a variety of emerging applications such as low-temperature oxidation of CO and Li-ion batteries [1,2]. The crystalline structure of Co_3O_4 is classified as a cubic (space group $Fd\bar{3}m$) where the transition metal Co exists in two distinct oxidation states according to the typical spinel formula AB_2O_4 (A-site = Co^{2+}, B-site = Co^{3+}). These divalent and trivalent cations exhibit the tetrahedral AO_4 and octahedral BO_6 coordination, respectively. Due to the crystal field theory, they are consequently in different local magnetic states. The divalent ions opt to be in a high-spin (HS) state coupling with four neighbors of the same kind by the anti-ferromagnetic (AFM) ordering. On the contrary, the trivalent ions adopt a low-spin (LS) state caused by the immense crystal-field splitting of 3*d* orbitals [3]. The presence of different magnetic states of cations in Co_3O_4 leads to the strong spin-lattice correlation, e.g., the AFM-to-FM transition below Néel temperature in nanostructured Co_3O_4, which is originated by the normal-to-inverse transformation [4,5]. As more examples, the underlying interplay between lattice and magnetism has been also reported in Cr-based spinels due to spin-phonon coupling [6,7]. In this context, one can expect sensitive magnetic properties upon structural changes induced by an external incentive, i. e., pressure.

An application of external pressure to solids consequently reduces interatomic distances to initiate profound changes in outer electron shells due to more overlapping, which directly influences chemical and physical properties [8]. Therefore, numerous novel phenomena are potentially emerged upon structural compression. In particular, pressurizing spinel compounds is able to alter their magnetic exchange interactions for the switching between AFM and FM configurations [9,10]. Magnetic transitions from the high-spin to low-spin upon compression have been reported for Fe_3O_4 spinel [11,12]. Pressure can also induce phase transition in spinels where the novel high-pressure phases usually exhibit the enhanced coordination number of cations and the differences in physical properties with respect to the initial spinel structures [13]. Thus, the physical properties of spinel compounds are effectively tunable by applying external pressure. In particular, if quenchable, high-pressure phases of Co_3O_4 may imply its improved catalytic properties.

The fundamental aims of this study are to elucidate the crystal structure and the electronic property of compressed Co_3O_4. A Previous study has shown a charge-transfer type transition from a normal-spinel to a partial inverse-spinel at 17.7 GPa [14]. Later, S. Hirai *et. al.* have argued that Co_3O_4 structurally gets transformed from a cubic (CB) to a lower-symmetry monoclinic (MC) phase (space group $P2_1/c$ no. 14) whose the onset is at 30 GPa and the complete phase transition occurs above 46 GPa [15]. In addition, there is an evidence that this high pressure phase can be quenchable to another monoclinic phase (space group $C2/m$ no. 12) at around 0.5 GPa. Being motivated by this debate, we have carried out *first-prinicples* theoretical investigation in order to acquire more descriptions of the phase transition and the underlying electronic property of the high-pressure phase. We have found the first-order phase transition in Co_3O_4 from $Fd\bar{3}m$ to $P2_1/c$ at 35 GPa, where the detailed crystal structure of high-pressure phase differs from the reported study [15]. The monoclinic phase $C2/m$ is not energetically favorable for the entire range of considered pressure. The CB-to-MC transition is attributed to the charge-transfer between the di- and trivalent cations via the enhanced 3*d*-3*d* interactions. The MC phase is a semiconductor with the reduced band gap compared with the starting CB.

[a] *Materials Theory Division, Department of Physics and Astronomy, Uppsala University, P.O Box 530, S75121, Uppsala, Sweden*

[b] *College of Civil Engineering and Mechanics, Yanshan University, Hebei 066004, China*

[c] *Applied Materials Physics, Departments of Materials and Engineering, Royal Institute of Technology (KTH), S-10044, Stockholm, Sweden*

2 Computational methods

In the present study, we have employed VASP code[16] to carry out a systematic study of the crystal structures, lattice dynamics, magnetic and electronic properties of Co_3O_4 under compression. The core-valence interactions were treated by projector-augmented wave (PAW) approach[17] with Co ($3p^6 3d^8 4p^1$) and O ($2s^2 2p^4$) being the valence states. The exchange-correlation functional was approximated according to generalized gradient approximation of Perder-Wang-Ernzerhof (PBE)[18], which is demonstrated to reliably deal with transition oxides at high pressure region due to the increase of bandwidth and screening[19,20]. The energy cut-off representing a plan-wave basis was chosen to be 1000 eV. For Brillouin zone integration, the k-point mesh of $8 \times 8 \times 8$ and $8 \times 4 \times 6$ was chosen for CB and MC respectively. Structural optimization was terminated when the Hellmann-Feynman forces exerting on each atom became less than 0.5 meV/Å with the electronic self-consistence energy less than 1×10^{-6} eV. Furthermore, phonon dispersions were calculated from a supercell of $2 \times 2 \times 2$ for CB and $3 \times 1 \times 2$ for MC by using PHONOPY program[21].

3 Results and discussion

The CB phase is characterized as a direct spinel structure, where the divalent cations occupy the A site 8*a*(0,0,0) and the trivalent ones completely reside in the B site 16*d*(0.625,0.625,0.625). If the B site is accommodated by both types of cations, the CB phase is called an inverse spinel. The O anions are located at (*u*,*u*,*u*), $u = 0.3881$[3]. The crystal structure of CB, depicted in figure 1(a), constitutes two types of polyhedral units, i. e., undistorted tetrahedra AO_4 and octahedra BO_6. The tetrahedra are connected with neighboring octahedra by linking the vertices, while the octahedra share the edges among themselves. Each oxygen belongs to three octahedra and one tetrahedra. The bond distances of A-A, A-B and B-B are found to be 3.52 Å, 3.37 Å and 2.88 Å, respectively. The A-O (B-O) bond distance is calculated to be 1.95 (1.93) Å, which displays less than 3 % deviation from the measured value of 1.935 (1.920) Å[15]. Our calculated crystallographic data of CB is assembled in table 1. The manifested consistency between our findings and previously reported studies validates the further investigations.

The CB phase is subsequently pressurized from 0 to 100 GPa. According to the spinel-type structures, the volumes of polyhedra and the cation-anion bond lengths can be empirically expressed in terms of the oxygen position *u* because the edges of polyhedra are made up of oxygen[22]. Thus, the variation of the parameter *u* with respect to pressure is able to explain the cation ordering under pressure[23]. Normal and inverse spinels respond differently to pressure because of the

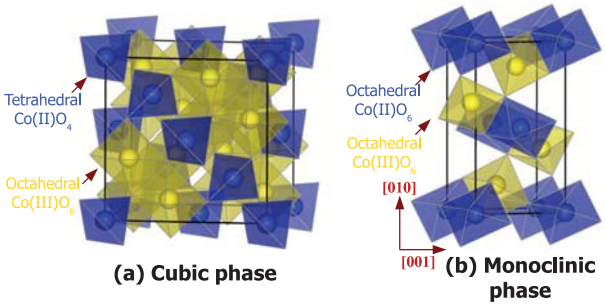

Fig. 1 Crystal structures of (a) cubic (CB) $Fd\bar{3}m$ and (b) monoclinic (MC) $P2_1/c$. The blue (yellow) polyhedra in CB represent AO_4 (BO_6), while those in MC denote AO_6 (BO_6).

different occupancies of cations at A and B sites. The former shows a gradual decrease in *u* with pressure, while the later behaves the reverse[23]. Figure 2(a) reveals that there is a monotonic reduction in *u* from 0 to around 23 GPa, which indicates that pressure does not result in the transition from normal to inverse spinel. Interestingly, a sudden drop is observed at around 27 GPa and it accounts for the significant change in the structure originated from the collapse of local magnetic moments of Co(II). Note that the magnetic moment of Co(III) is calculated to be 0.00 μ_B at 0 GPa and it remains zero upon increasing pressure. The disappearance of magnetic moments is attributed to the shortening of Co-O bond distances at high pressure due to the bandwidth broadening[19]. Therefore, the CB phase becomes nonmagnetic at the onset pressure of 27 GPa.

In the CB lattice, Co(III) cations are diamagnetic owing to the strong crystal field splitting[3]. On the contrary, Co(II) cations at the 8*a* position form two face-centered cubic (fcc) sub-lattices having the origins at (0,0,0) and (0.25,0.25,0.25). Each spin of Co(II) ion at (0,0,0) is oppositely aligned with the spins from four neighbors at (0.25,0.25,0.25). The CB phase is regarded as the anti-ferromagnetic (AFM) ordering with the super-exchange interactions through the favorable path Co(II)-O-Co(III)-O-Co(II)[3]. The direct exchange interactions between Co(II) are negligible because of the large bond length. Our total-energy calculation shows that the AFM ordering is more favorable than the FM state, agreeing with an experimental finding[3]. During the compression, we find the AFM state is energetically retained (as shown in figure 3) until the vanishing of magnetic moment at 27 GPa. It has been reported that the AFM ordering is closely associated with the empty e_g states of Co(III) as evidenced by the variation in Néel temperature with respect to different B-site cations such as $CoAl_2O_4$ (4 K), $CoRh_2O_4$ (27 K) and $CoGa_2O_4$ (10 K)[24–26]. Therefore, the negligible change in the magnetic moment of Co(III) with pressure can be relevant to the maintenance of

Table 1 The calculated crystallographic parameters and atomic coordinates of CB at ambient pressure and MC phase at 38 GPa. The experimental values of CB are from ref.[3,14].

Space group	Lattice parameters (Å)	B_0 (GPa)	B_0'	Atom	Fractional coordinates
$Fd\bar{3}m$ (227)	8.104	207	4.6	Co1(8*a*)	0.0000
$Z = 8$	8.065[14]	199[14]		Co2(16*d*)	0.6250
				O(32*e*)	0.3874
					0.3881[3]
$P21/c$ (14)	2.725, 8.893, 4.674	202	4.3	Co1(2*a*)	0.000
$Z = 2$	β = 108.85			Co2(4*e*)	0.7604, 0.3529, 0.9736
				O1(4*e*)	0.3678, 0.4527, 0.2145
				O2(4*e*)	0.0705, 0.1854, 0.1911

AFM state. Another explanation is that pressure strengthens the AFM ordering owing to the reduction in Co(II)-Co(II) distance that Néel temperature has been shown to be enhanced with increasing pressure[27]. In addition, Jahn-Tellor distortion of the tetrahedra and octahedra is not observed during the compression, indicating that the compression of CB still preserves the crystal field symmetry. Figure 2(b) shows that tetrahedral AO_4 is more compressible than octahedral BO_6, which reflects the stiffer bonds of higher oxidation state[23] and signifies that the higher coordination number of C(II) cations in the high-pressure phase of Co_3O_4 is expected.

By considering enthalpy, further compressing the CB phase leads to the first-order phase transition to the MC phase with space group $P2_1/c$ (No. 14) at 35 GPa as indicated in figure 2(c). The calculated transition pressure lies within the experimental value (i. e., 30 - 46 GPa)[15], but it is less than the pressure (41.2 GPa) at which the CB phase has been experimentally proposed to retain[14]. However, it is generally known that the transition pressure is functional dependent. In particular, PBE has been reported to underestimate the transition pressure in some cases[28–30]. The CB-to-MC transformation apparently occurs after the local high-spin to low-spin phase transition and it is accompanied by the relative contraction of volume by around -6.1 %. The MC phase, shown in figure 1(b), contains two types of polyhedra namely $Co(II)O_6$ and $Co(III)O_6$ and it is open and layered along the [001] direction. The octahedra are interconnected to each other by sharing edges, which displays a direct consequence of the increased coordination number of Co(II) from 4 in CB to 6 in MC. As a result, the cation-cation bond distances become nearly the same; A-A = 2.73 Å, A-B = 2.68 Å and 2.73 AA. These notably differ from those in CB where A-A >A-B >B-B. Furthermore, these shortened bonds compared with those in the CB phase yield the enhanced interactions between the cations. The AO_6 and BO_6 polyhedra are highly distorted with the average A-O and B-O bond distances of 1.89 Å and 1.92 Å, respectively. The bulk modulus (B_0) and its first derivative (B_0') of MC are estimated to be 202 GPa and 4.3, which are respectively comparable to 207 GPa and 4.6 of CB.

It is noted that the crystal structures of Co_3O_4 at high pressure have been questionable owing to anisotropic crystal structure that the atomic positions are assigned to the those of isostructural compounds[15]. In spite of the CB-to-MC transition, our calculated crystal parameters of MC phase presented in table 1 differ from those of previous study where a = 4.1928 Å, b = 3.0462 Å, c = 8.685 Å, β = 95.05[15]. In addition, the emergence of another monoclinic phase (MC-I) of space group $C2/m$ (no. 12) in the pressure range 28.0 to 0.5 GPa during pressure release has been proposed by the experimental study[15]. However, this phase, where Co(II) and Co(III) have octahedral coordination by O atoms, is not energetically found in our calculation, because its formation enthalpy is relatively greater than the CB and MC phases.

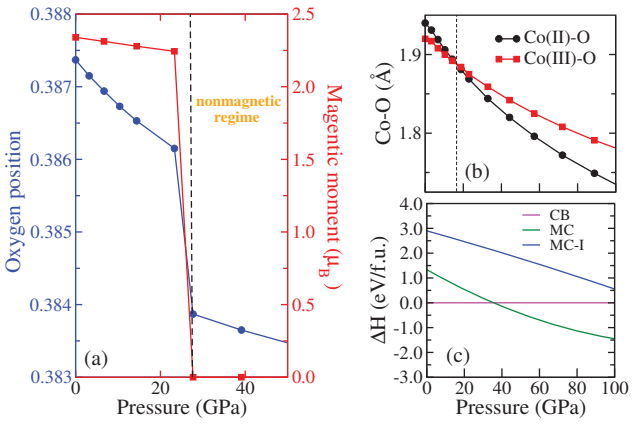

Fig. 2 (a) variation of oxygen position and the local magnetic moment of Co(II) of CB as a function of pressure (b) the pressure dependence of Co-O bond lengths of CB and (c) the relative enthalpy as a function of pressure, referenced to CB.

For the assessments of dynamical stability, figure 4 shows the phonon dispersion and corresponding phonon density of state (PDOS) of CB at 0 and 46 GPa and MC at 46 GPa.

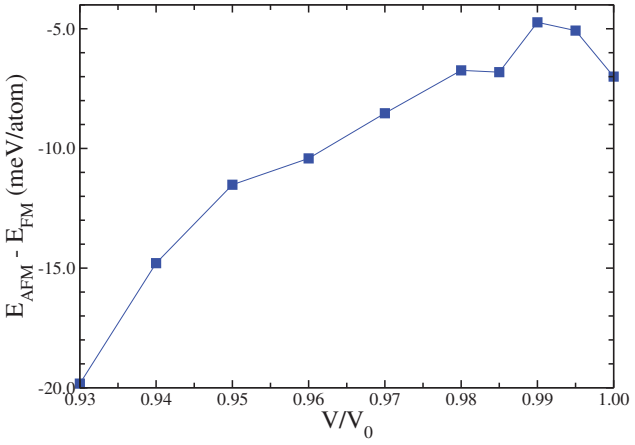

Fig. 3 The comparison of total energy of CB phase in AFM and FM state. Here, V_0 represents the equilibrium volume at 0 GPa.

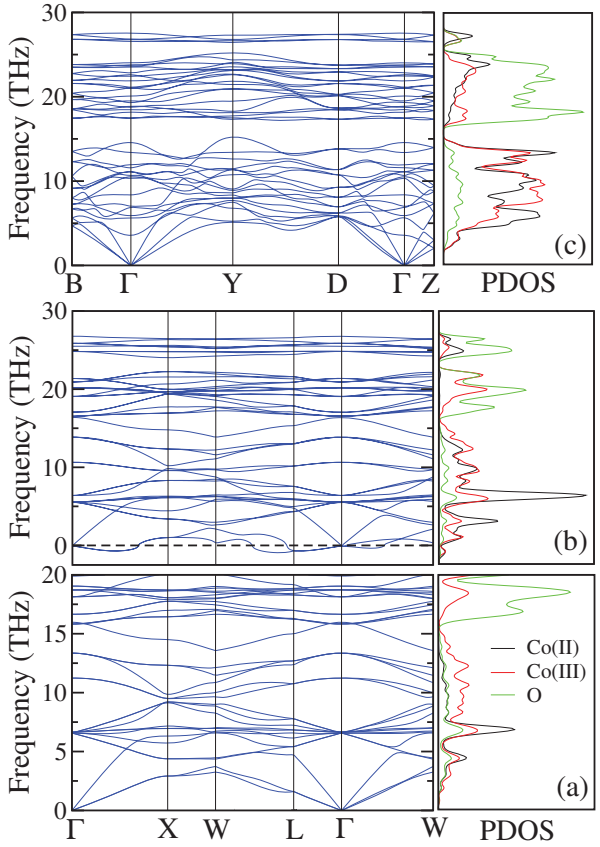

Fig. 4 Phonon dispersion and corresponding density of states (PDOS) of (a) CB at ambient pressure (b) CB at 46 GPa and (c) MC at 46 GPa. The unit of PDOS is states per ion.

For CB at 0 GPa, the low-frequency regime is predominantly originated from Co(II) vibration, whereas the high-frequency range is mainly derived from the Co(III)-O vibration due to stiffer Co(III)-O bonds. At 46 GPa, there are soft phonon modes coming from the mixture of Co(II) and Co(III) vibration. Note that imaginary modes are expected to be originated from Co(II) because of its major change in coordination number at increasing pressure. However, the structural instability contributed by both types of cations is due to charge transfer between Co(II) and Co(III) cations at high pressure [14]. For the MC phase, the phonon dispersion at 46 GPa shows the absence of imaginary modes, confirming its dynamical stability. The vibrational frequency is apparently divided into two parts where the low to medium range is contributed almost equally by vibration of Co(II) and Co(III). This reveals the enhanced interactions between neighboring Co cations at high pressure, which are responsible for the volume discontinuity in the first-order phase transition of this material. Furthermore, the drastic increase in vibration at high frequency is observed due to the shorter Co-O bond lengths with high oxygen bonding energies.

For the analysis of electronic structures, the orbitally projected density of states (DOS), calculated by the hybrid functional HSE06, is depicted in figure 5. From figure 5(a), one can see that Co(II) ions in the CB phase at 0 GPa adopt a high-spin (HS) $e_g^4 t_{2g}^3$ (S = 3/2) state due to the strong exchange splitting. On the other hand, Co(III) ions experience the smaller exchange splitting than the crystal-field splitting, resulting in a low-spin (LS) $t_{2g}^6 e_g^0$ (S = 0) configuration. The significant hybridization between Co(III)-3*d* and O-2*p* near the Fermi level yields a shorter Co(III)-O bonds than Co(II)-O bonds. The calculated band gap at Γ is 3.1 eV, comparable with 3.25 eV by PBE + U [31]. On the other hand, the DOS of MC at 46 GPa, shown in figure 5(b), reveals that the MC phase is a non-magnetic semiconductor with the reduced band gap of 1.8 eV. It is seen that the MC phase shows a covalent character because of the increasing hybridization between Co cations, i. e., the charge transfer between Co(II) and Co(III) [14]. In addition, the narrow bands highlighted by the dotted ellipse emerge right below the valence band edge and they are derived from Co-3*d* and O-2*p* states. This is because the shrunk Co(II)-Co(III) bond distances and the edge sharing of Co(II)O_6 and Co(III)O_6 octahedra in the MC phase. In other words, the strong localization states arise from the enhanced interactions between the Co cations passed by the sharing of O atoms. It is therefore possible to establish that the pressure-induced phase transition is governed by the charge transfer between di- and trivalent cations via the $3d - 3d$ interactions.

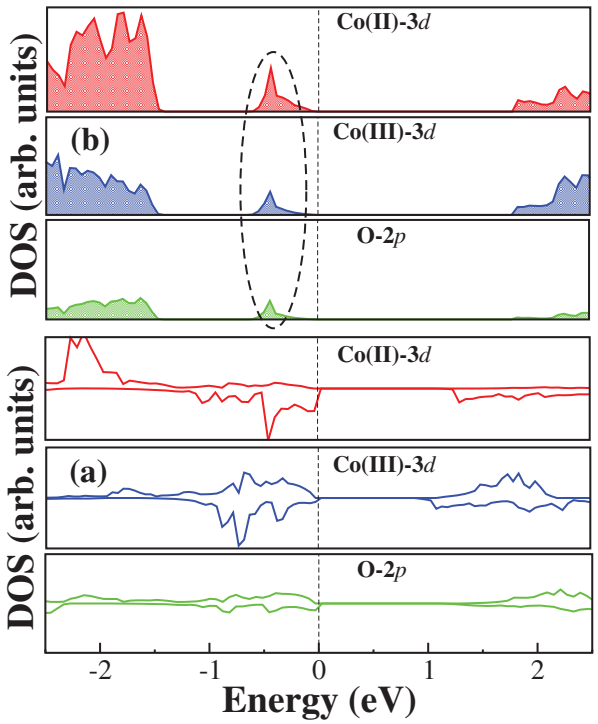

Fig. 5 Orbital-projected density of states (DOS) of 3*d*-orbitals of Co^{2+}, Co^{3+} and O: (a) CB at ambient pressure and (b) MC-I at 38 GPa. The Fermi energy is shifted to zero.

4 Conclusions

To summarize, we have explored the pressure-driven phase transitions in Co_3O_4 spinel by theoretical approaches based on first-principles DFT. We calculate the transition pressure from cubic (CB) $Fd\bar{3}m$ to monoclinic (MC) $P2_1/c$ to be at 35 GPa, occurring after the local high-spin to low-spin phase transition. The high-pressure phase exhibits the octahedral coordination of Co(II) and Co(III), whereas the CB phase contains fourfold coordination of Co(II) and sixfold coordination of Co(III). The phonon dispersion reveals the dynamical instability of the CB phase above the transition pressure where the MC phase correspondingly becomes stable. The high-pressure phase is a non-magnetic semiconductor with the band gap of 1.8 eV. The phase transition is attributed to charge transfer between cations via the enhanced 3*d*-3*d* interactions. The monoclinic phase $C2/m$ is found energetically unfavorable for the entire range of considered pressure. Our work can stimulate further investigations on this phase because it has been proposed to exist at low pressure and may benefit catalytic activity of this material.

T. Kaewmaraya acknowledges the Commission on Higher Education (CHE) of Thailand via the Strategic Frontier Research (SFR) Scheme for the financial support. X. Yang acknowledges the China Scholarship Council for funding his PhD study. W. Luo and R. Ahuja acknowledge the Swedish Research Council (VR) for the financial support. The Swedish National Infrastructure for Computing (SNIC) at NSC (Matter and Triolith clusters) at Umeå (Abisko and Akka clusters) provides computing facilities for this project.

References

1 X. W. Xie, Y. Li, Z. Q. Liu, M. H. M. and W. J. Shen, *Nature*, 2009, **458**, 746–749.
2 D. Liu, X. Wang, X. Wang, W. Tian, Y. Bando and D. Golberg, *Sci. Rep*, 2013, **3**, 2543.
3 W. L. Roth, *J. Phys. Chem. Solids*, 1964, **25**, 1–10.
4 W. Chen, C. Chen and L. Guo, *J. Appl. Phys.*, 2010, **108**, 073907.
5 S. K. Meher and G. R. Rao, *J. Phys. Chem. C*, 2011, **115**, 25543.
6 J. Hemberger, T. Rudolf, H.-A. K. von Nidda, F. Mayr, A. Pimenov, V. Tsurkan and A. Loidl1, *Phys. Rev. Lett.*, 2006, **97**, 87204.
7 T. Rudolf, C. Kant, F. Mayr, J. Hemberger, V. Tsurkan and A. Loidl, *Phys. Rev. B*, 2007, **97**, 87204.
8 P. F. McMillan, *Chem. Rev. Soc.*, 2006, **35**, 855–857.
9 Y. Jo, J. G. Park, H. C. Kim, W. R. II and S.-W. Cheong, *Phys. Rev. B*, 2005, **72**, 184421.
10 H. Ueda and Y. Ueda, *Phys. Rev. B*, 2008, **77**, 224411.
11 S. Ju, T. Y. Cai, H. S. Lu and C. D. Gong, *J. Am. Chem. Soc.*, 2012, **134**, 13780–13786.
12 Y. Ding, D. Haskel, S. G. Ovchinnikov, Y. C. Tseng, Y. S. Orlov, J. C. Lang and H. K. Mao, *Phys. Rev. Lett.*, 2008, **100**, 045508.
13 F. J. Manjon, I. Tiginyanu and V. Ursaki, *Pressure-induced phase transitions on AB_2X_4 chalcogenide compounds*, Springer, 2014.
14 L. Bai, M. Pravica, Y. Zhao, C. Park, Y. Meng, S. V. Sinogeikin and G. Shen, *J. Phys.: Condens. Matter*, 2012, **24**, 435401.
15 S. Hirai and W. L. Mao, *Appl. Phys. Lett.*, 2013, **24**, 041912.
16 J. Hafner, *J. Comput. Chem.*, 2008, **29**, 2044–2078.
17 P. E. Blochl, *Phys. Rev. B*, 1994, **50**, 17953.
18 J. P. Perdew, K. Burke and M. Ernzerhof, *Phys. Rev. Lett.*, 1996, **77**, 3865.
19 R. E. Cohen, I. I. Mazin and D. G. Isaak, *Science*, 1997, **275**, 654–657.
20 Z. Fang, I. V. Solovyev, H. Sawada and K. Terakura, *Phys. Rev. B*, 1999, **59**, 762.
21 A. Togo, F. Oba and I. Tanaka, *Phys. Rev. B*, 2008, **78**, 34106.
22 R. J. Hill, J. R. Craig and G. V. Gibbs, *Phys. Chem. Miner.*, 1979, **4**, 317.
23 J. M. Recio, R. Franco, A. M. Pendas, M. A. Blanco, L. Pueyo and R. Pandey, *Phys. Rev. B*, 2001, **63**, 184101.
24 W. L. Roth, *J. Phys.*, 1964, **25**, 507.
25 G. Blasse, *Phys. Lett.*, 1965, **19**, 110.
26 D. Fiorani and S. Viticoli, *Solid Stat. Com.*, 1978, **25**, 155.
27 Y. Ikedo, J. Sugiyama, H. Nozaki, K. Mukai, H. Itahara, P. L. Russo, D. Andreica and A. Amato, *Physica B*, 2009, **404**, 652.
28 C. Cazorla, S. Binnie, D. A. é and M. J. Gillan, *High Pressure Research*, 2008, **28**, 449.
29 N. Yedukondalu, V. D. Ghule and G. Vaitheeswaran, *J. Chem. Phys.*, 2013, **138**, 174701.
30 W. Lee and X. Yao, *Comput. Mater. Sci.*, 2015, **106**, 76.
31 J. Chen, X. Wu and A. Selloni, *Phys. Rev. B*, 2011, **83**, 245204.